



 Cite this: *RSC Adv.*, 2021, 11, 17755

Highly-efficient red-to-yellow/green upconversion sensitized by phthalocyanine palladium with high triplet energy-level†

 Kai Wang,‡ Suqin Huang,‡ Ping Ding, Zuoqin Liang, Shuoran Chen,  Lin Li, Changqing Ye* and Xiaomei Wang *

Soluble 3,7,11,15-tetra(*tert*-butyl)phthalocyanine palladium (TBPCd) and 3,7,11,15-tetra(pentyloxy)phthalocyanine palladium (POPCd) were synthesized and employed as sensitizers in expectation of achieving red-to-yellow/green upconversion (UC), doped with rubrene (Rub) and 9,10-bis(phenylethynyl)anthracene (BPEA), respectively. Under excitation of a 655 nm diode laser ($\sim 1.5 \text{ W cm}^{-2}$), a maximum red-to-green UC efficiency of 0.07% and a maximum red-to-yellow UC efficiency of 8.03% were obtained and the latter can drive a Si-photodiode to generate obvious photocurrent. The results showed that although a large triplet energy-level difference ($\Delta E = {}^3E_{\text{sen.}} - {}^3E_{\text{anni.}}$) of the sensitizer (${}^3E_{\text{sen.}}$)/annihilator (${}^3E_{\text{anni.}}$) pair helps to improve the upconversion, the sensitizer/annihilator pair with a ΔE value less than zero still works. However, when the $\Delta E \leq -0.05 \text{ eV}$, this bicomponent pair is not valid anymore. Thus, a comparison of the ΔE value can predict whether the sensitizer/annihilator pair is useful, which presents a quantitatively evaluated approach for exploring new-type upconversion systems for the first time.

Received 31st March 2021

Accepted 4th May 2021

DOI: 10.1039/d1ra02528g

rsc.li/rsc-advances

1 Introduction

Triplet-triplet annihilation upconversion (TTA-UC), which is the observation of emission at higher energy (shorter wavelength) under the excitation of lower energy (longer wavelength), has attracted much attention owing to its potential applications for TTA-UC integrated dye-sensitized solar cells (DSSC),^{1–7} and photoelectrochemistry.^{8,9} Concretely, TTA-UC is facilitated by selective excitation of a strongly absorbing sensitizer in a longer wavelength region that internally converts to the triplet excited state; the triplet-triplet energy transfer (TTT) then occurs from the sensitizer to the annihilator and finally produces one single excited state between two annihilators (TTA), the latter thus emitting upconversion fluorescence.¹⁰ For the purpose of solar energy applications, the upconversion of the near infrared (NIR) to the visible light is attractive due to its making the best of harvesting the sunlight. Therefore, highly-efficient sensitizers in the NIR region are of importance. Fortunately, metallated phthalocyanine complexes (MPcs) are possibly one of the most suitable NIR triplet sensitizers because their Q bands of absorption are just right in the

near infrared (NIR) region and have high molar absorbance coefficients.¹¹ However, the MPcs as sensitizer are actually seldom reported yet.¹² The reasons are possibly owing to the poor solubility of the MPcs without substitution groups; on the other hand, the soluble MPcs with long flexible alkyl chain substitution are needed heavy and complicated synthesis procedures.

In this work, three phthalocyanine complexes: phthalocyanine palladium (PcPd), 3,7,11,15-tetra(*tert*-butyl)phthalocyanine palladium (TBPCd) and 3,7,11,15-tetra(pentyloxy)phthalocyanine palladium (POPCd) were synthesized by one-pot method (see ESI section, Fig. S1–S8, ESI†). The results showed that phthalocyanine complexes (TBPCd and POPCd) with peripheral short alkyl chains are soluble in common organic solvents, while phthalocyanine palladium (PdPc) is insoluble. So, the two soluble TBPCd and POPCd were used as sensitizers, doped with rubrene (Rub) and 9,10-bis(phenylethynyl)anthracene (BPEA), respectively to obtain TBPCd/Rub, TBPCd/BPEA, POPCd/Rub and POPCd/BPEA pairs. Under the excitation of 655 nm diode laser, the UC efficiency and related triplet energy-level difference ($\Delta E = {}^3E_{\text{sen.}} - {}^3E_{\text{anni.}}$) of sensitizer (${}^3E_{\text{sen.}}$)/annihilator (${}^3E_{\text{anni.}}$) pair were investigated.

2 Experimental section

2.1 Materials and upconversion solutions

All chemicals used in the synthesis, with the exception of usual solvents and reagents, were purchased from Acros and Aldrich Co. and used without further purification. Annihilators rubrene (Rub) and 9,10-bis(phenylethynyl)anthracene (BPEA) were

Suzhou Key Laboratory of Flexible & Printing Optoelectronic Materials, School of Materials Science and Engineering, Suzhou University of Science and Technology, Suzhou, 215009, China. E-mail: yechangqing@mail.usts.edu.cn; wangxiaomei@mail.usts.edu.cn

† Electronic supplementary information (ESI) available. See DOI: 10.1039/d1ra02528g

‡ These authors contributed equally to this work.



purchased from J&K Scientific Ltd. Palladium phthalocyanines (**PcPd**, **TBPcPd** and **POPcPd**) were synthesized and characterized in our lab (see ESI section†).

Four sensitizer/annihilator pairs (**TBPcPd/Rub**, **TBPcPd/BPEA**, **POPcPd/Rub** and **POPcPd/EBPEA**) with different concentration ratios were prepared in toluene and kept in the dark prior to measurements.

2.2 TTA-UC measurements

Absorption and fluorescence spectra were measured with a Hitachi U-3500 spectrophotometer and FLS920 Edinburgh fluorophotometer, respectively. The UC spectra was recorded with PR655 SpectraScan colorimeter under the excitation of 655 nm diode laser. The sensitizer/annihilator pair in toluene were degassed for 15 min before measurement. The UC efficiency (Φ_{UC}) was calculated by eqn (1),¹⁰

$$\Phi_{UC} = 2\Phi_r \left(\frac{A_r}{A_s}\right) \left(\frac{F_s}{F_r}\right) \left(\frac{\eta_s}{\eta_r}\right)^2 \quad (1)$$

where A_r and A_s are the absorbance of the reference (ZnPc) and sensitizer at the excitation wavelength (655 nm), respectively. F_s and F_r stand for the integrated UC of annihilator and integrated fluorescence of ZnPc, respectively. Φ_r is the fluorescence quantum yield of ZnPc (20% in DMSO).¹³ η_s and η_r are the refractive index of sensitizer/annihilator solution and ZnPc solution (to simplify, η_s and η_r are the refractive index of toluene and DMSO). The equation is multiplied by a factor of 2, accounting for the fact that two absorbed photons are required to produce one up converted photon. Thus, the various parameters based on the eqn (1) above are presented in Table S1.†

3 Results and discussion

3.1 Absorption and photoluminescence

Molecular structures of palladium phthalocyanines (**PcPd**, **TBPcPd** and **POPcPd**) and annihilators (**Rub** and **BPEA**) are shown in Fig. 1. As can be seen that **TBPcPd** and **POPcPd**

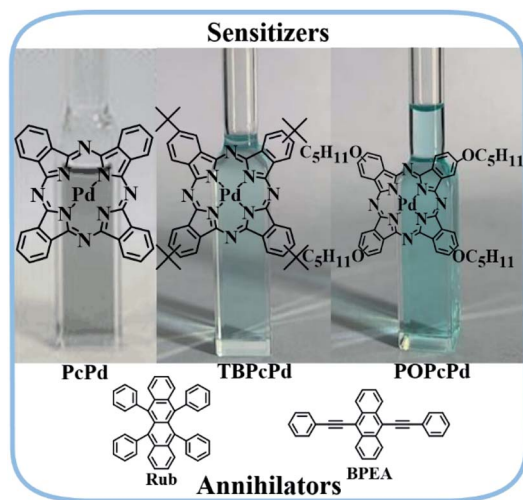


Fig. 1 Molecular structures of palladium phthalocyanines (**PcPd**, **BPCPd** and **POPcPd**) and annihilators (**BPEA** and **Rub**) as well as the photographs of three MPCs dispersed in toluene (10 μ M).

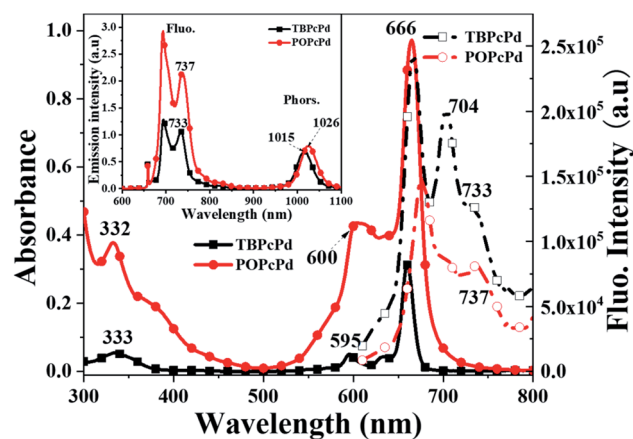


Fig. 2 Absorption (left), fluorescence (right) and phosphorescence (inset) spectra of **TBPcPd** and **POPcPd** in toluene at 10 μ M (fluorescence spectra were measured under the excitation of 655 nm Xe lamp while phosphorescence spectra (inset) were obtained under the excitation of 655 nm diode laser, N_2 atmosphere and room temperature).

modified with substituents show better solubility, while **PcPd** without substituents is insoluble. Thus, both **TBPcPd** and **POPcPd** can act as sensitizers in toluene. As shown in Fig. 2, the maximum Q-bands of **TBPcPd** and **POPcPd** are located at 666 nm with the absorption edge near to 700 nm (**TBPcPd**) or beyond 700 nm (**POPcPd**). Relative to **TBPcPd**, **POPcPd** presents redshift both in absorption spectrum and fluorescence spectrum. We noticed that the phosphorescence peaks of **TBPcPd** and **POPcPd** are located at 1015 nm and 1026 nm, respectively (see Fig. 2, inset). Thus, the triplet energy levels of **TBPcPd** (${}^3E_{sen} = 1240/1015$ nm) and **POPcPd** (${}^3E_{sen} = 1240/1026$ nm) are calculated at 1.222 eV and 1.209 eV, respectively.

As for annihilator, **BPEA** exhibits dual absorption bands (438 nm and 457 nm) and two intensive fluorescence peaks located at 477 nm and 508 nm. **Rub** shows three absorption bands (460–560 nm) and fluorescence peaks at 556 nm and 600 nm (Fig. 3). All the optical properties of sensitizers (**TBPcPd**

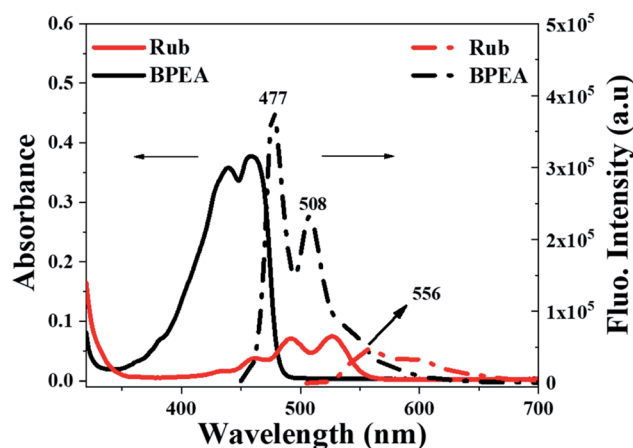


Fig. 3 Absorbance and emission spectra of **BPEA** and **Rub** in toluene (10 μ M) under the excitation of respective maximum absorption.



Table 1 The optical properties and the triplet energy-levels of sensitizers and annihilators (solvent: toluene, 10 μM)

Sensitizer	λ_{abs} (nm)	λ_{p} (nm)	$^3E_{\text{sen.}}$ (eV)	
TBPCd	333 (B), 632–660 (Q)	1015	1.222	
POPCd	332, 380 (B), 600–666 (Q)	1026	1.209	
Annihilator	λ_{abs} (nm)	λ_{f} (nm)	Φ_{f}	$^3E_{\text{anni.}}$ (eV)
Rub	460–526	556, 600	98%	1.140 (ref. 14)
BPEA	438, 457	477, 508, 545	86%	1.260 (ref. 15)

and **POPCd**) and annihilators (**Rub** and **BPEA**) as well as the triplet energy-levels ($^3E_{\text{sen.}}$ and $^3E_{\text{anni.}}$) are presented in Table 1.

3.2 TTA upconversion performances

Herein, we employed 655 nm red laser as the excitation light source due to lack of the NIR laser. When the **TBPCd/Rub** and **TBPCd/BPEA** pairs in degassed toluene were irradiated by the 655 nm diode laser ($\sim 1.5 \text{ W cm}^{-2}$), respectively, the red-to-yellow UC from **TBPCd/Rub** (optimized concentration ratio: 14 $\mu\text{M}/1.2 \text{ mM}$) pair and red-to-green UC from **TBPCd/BPEA** (optimized concentration ratio: 10 $\mu\text{M}/5 \text{ mM}$) pair were recorded (Fig. S9 and S10[†]). Power-dependent upconversion spectra

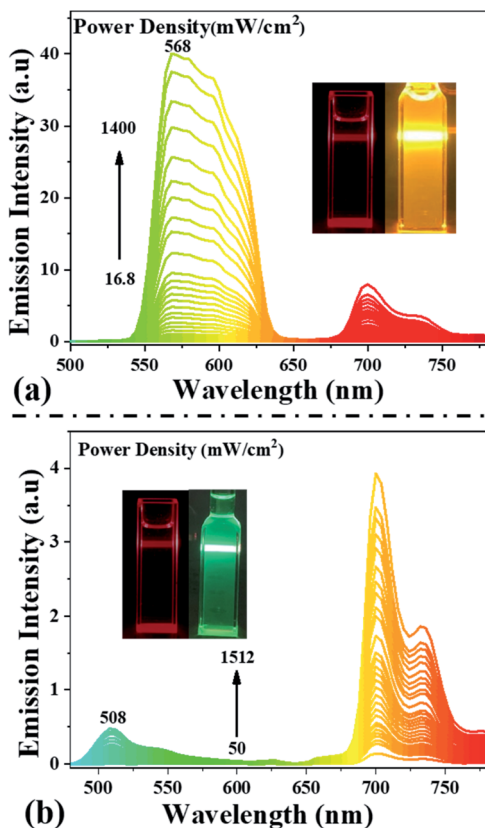


Fig. 4 Power-dependent upconversion of **TBPCd/Rub** (a) and **TBPCd/BPEA** (b) as well as the photographs with 655-filter (inset) in deaerated toluene at 655 nm excitation, ([**TBPCd**]/[**Rub**]: 14 $\mu\text{M}/1.2 \text{ mM}$, [**TBPCd**]/[**BPEA**]: 10 $\mu\text{M}/5 \text{ mM}$).

(Fig. 4) showed that both upconversion show rapidly enhanced with the anti-Stokes shifts ($E_{\text{UC}} - E_{\text{ex}}$) at 0.32 eV for red-to-yellow (568 nm) (Fig. 4a) and at 0.58 eV for red-to-green (508 nm) (Fig. 4b). We noticed that the red-to-yellow UC intensity showed much stronger than red-to-green UC. The former efficiency (Φ_{UC}) was calculated at 8.03% and later at 0.07% (Fig. S11 and Table S1, ESI[†]).

TTA-UC efficiency (Φ_{UC}) is mainly dependent of two quantum processes: the triplet-triplet energy transfer (TTT) and the triplet-triplet annihilation (TTA). The TTT process can be evaluated by the Stern–Volmer equation: $P_0/P = K_{\text{sv}}[Q] + 1 = k_{\text{q}} \times {}^3\tau \times [Q] + 1$,¹⁶ where P_0/P is the ratio of the phosphorescence of sensitizer without and with annihilator. $[Q]$ and K_{sv} are the molar concentration of annihilator and the Stern–Volmer constant, respectively. ${}^3\tau$ is the phosphorescence lifetime of sensitizer; k_{q} is the quenching constant that can represent the TTT process.¹⁷ So, the phosphorescence intensity of **TBPCd** quenched by **Rub** or **BPEA**, respectively, was measured (Fig. S12 and S13, ESI[†]) and the results are presented in Fig. 5a (curve i, ii). Clearly, **TBPCd/Rub** pair possesses much larger K_{sv} value (5.26 mM^{-1}) than **TBPCd/BPEA** pair (3.09 mM^{-1}). For the given sensitizer **TBPCd** (${}^3\tau$ is the same), larger K_{sv} value means larger the quenching constant (k_{q}) of the TTT process. Therefore, TTT process of **TBPCd/Rub** pair is more efficient than **TBPCd/BPEA** pair.

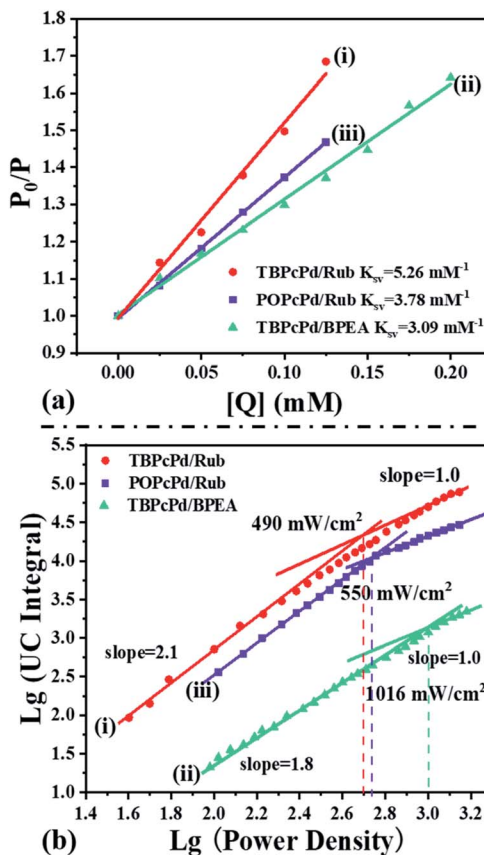


Fig. 5 Stern–Volmer curves (a) and the plots of upconversion integral versus power density (b) of **TBPCd/Rub**, **TBPCd/BPEA** and **POPCd/Rub** upon excitation at 655 nm.



Table 2 Parameters of different sensitizer/annihilator pairs in degassed toluene at the respective optimized concentration ratio

Sen./anni.	λ_{UC} (nm)	$E_{UC}-E_{ex}$ (eV)	K_{SV} (mM ⁻¹)	I_{th} (mW cm ⁻²)	ΔE (eV)	Φ_{UC} (%)
TBPCd/Rub	568	0.32	5.65	490	0.082	8.03
POPCd/Rub	568	0.32	3.64	550	0.069	1.83
TBPCd/BPEA	508	0.58	2.83	1016	-0.038	0.07
POPCd/BPEA	—	—	—	—	-0.051	—

On the other hand, the triplet-triplet annihilation process (TTA) could be estimated by the plot of UC integral *versus* the excited power. As presented in Fig. 5b (curve i, ii), there are two different straight lines with slope ~ 2 and ~ 1 . The former stands for the unsaturated stage of TTA while the later for the saturated one.^{18,19} The crossing point of both lines is defined as the threshold value (I_{th}),^{19,20} that is, the lowest excitation intensity is required for the most effective TTA process. Thus, the I_{th} value of **TBPCd/Rub** pair (490 mW cm⁻²) is almost twice smaller than that of the **TBPCd/BPEA** pair (1016 mW cm⁻²), indicating that the former possesses more efficient TTA than the latter. Clearly, both TTT (evaluated by K_{sv}) and TTA (evaluated by I_{th}) of **BPCd/Rub** pair are more efficient than those of **TBPCd/BPEA** pair.

Under the identical measurement conditions, **POPCd/Rub** presents the red-to-yellow UC with the efficiency (Φ_{UC}) at 1.84%, along with the Stern-Volmer constant ($K_{sv} = 3.78$ mM⁻¹) and threshold excitation intensity ($I_{th} = 550$ mW cm⁻²), as shown in Fig. S14-S16, ESI† Fig. 5a (curve iii) and Fig. 5b (curve iii). However, the **POPCd/BPEA** pair has not been observed the upconversion phenomenon (Fig. S14, ESI†). All related UC performance parameters of different sensitizer/annihilator pairs are presented in Table 2.

Further analysis found that the UC efficiency (Φ_{UC}) is strongly dominated by the triplet energy-level difference ($\Delta E = {}^3E_{sen.} - {}^3E_{anni.}$) of sensitizer (${}^3E_{sen.}$)/annihilator (${}^3E_{anni.}$) pair, since sensitizer with higher ${}^3E_{sen.}$ value than annihilator (${}^3E_{anni.}$) can ensure the former triplet energy transfer top-down to the latter^{21,22} and then the subsequent TTA. As shown in Fig. 6a, under the excitation of 655 nm, the sensitizer **TBPCd** reaches the triplet excited state (T_1) *via* intersystem crossing (ISC). Since the ${}^3E_{sen.}$ value of **TBPCd** (1.222 eV) is 0.082 eV higher than **Rub** (${}^3E_{anni.} = 1.140$ eV),¹⁴ this TTT process is efficient and resultly produces abundant triplet ${}^3Rub^*$ molecules for TTA process. Therefore, the UC efficiency of **TBPCd/Rub** pair is as high as 8.03%. For **POPCd/Rub** pair, the ΔE value (${}^3E_{sen.} - {}^3E_{anni.} = 1.209$ eV - 1.14 eV) is at 0.069 eV (lower than the **TBPCd/Rub** pair). Accordingly, the UC efficiency of **POPCd/Rub** pair is dramatically reduced to 1.84% (Fig. 6b).

Noted that the ${}^3E_{sen.}$ value of **TBPCd** is lower than the ${}^3E_{anni.}$ value of **BPEA** (${}^3E_{anni.}$), where such triplet-triplet energy transfer (TTT) can occur from the bottom up. As shown in Fig. 6c, the ΔE value of **TBPCd/BPEA** pair is equal to -0.038 eV, the red-to-green upconversion can also be observed with the efficiency at 0.07%. However, when the ΔE value of **POPCd/BPEA** pair is equal to -0.051 eV, the UC cannot happen anymore (Fig. 6d and S14, ESI†). Therefore, a comparison of the triplet energy-levels of sensitizer and annihilator can predict whether the

upconversion system works, which can provide a simple evaluated approach for exploring the new-type upconversion sensitizers.

3.3 TTA-UC application

The potential prospect toward TTA-upconversion can be applied in upconversion-powered solar-cell. Here, the silicon diode (photosensitive area at 9 mm²) was integrated with red-to-yellow upconversion pair (**TBPCd/Rub** solution, $\Phi_{UC} = 8.03\%$) that is irradiated by a diode solid state laser (655 nm, ~ 1.5 W cm⁻²). The yellow upconverted photons radiated by the **TBPCd/Rub** solution can be absorbed by Si-diode that is placed near the quartz cuvette, as shown in Fig. 7 (inset). To confirm that the photocurrent of Si-diode was indeed induced by the yellow upconversion, a short-pass filter (<650 nm) was placed between the red laser and the quartz cuvette in order to eliminate wavelengths longer than 650 nm.

Thus, the photocurrent curve generated by the **TBPCd/Rub** solution can be recorded by a computer controlled Keithley-4200 power meter (as shown in Fig. 7, blue solid line (d)). As can be seen that the current density of short circuit (J_{sc}) and voltage of open circuit (V_{oc}) obtained from **TBPCd/Rub** are at 9.7 mA cm⁻² and 0.47 V, indicating that TTA red-to-yellow upconversion and solar-cell integration have potential applications.

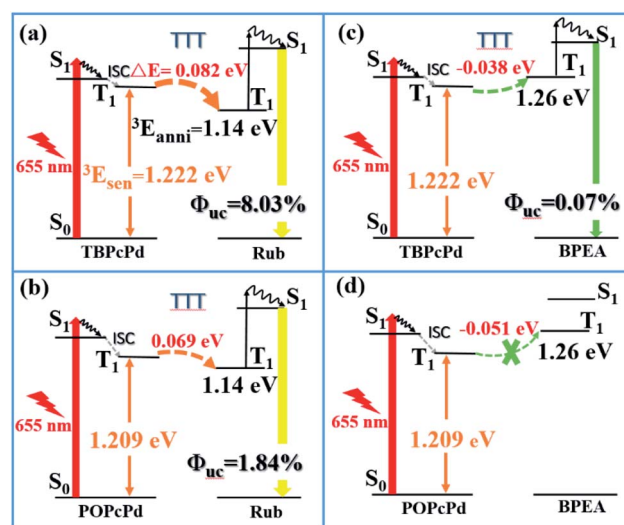


Fig. 6 The influence of triplet energy-level difference ($\Delta E = {}^3E_{sen.} - {}^3E_{anni.}$) upon the TTA-UC efficiency ((a) **TBPCd/Rub**; (b) **POPCd/Rub**; (c) **TBPCd/BPEA**; (d) **POPCd/BPEA**).



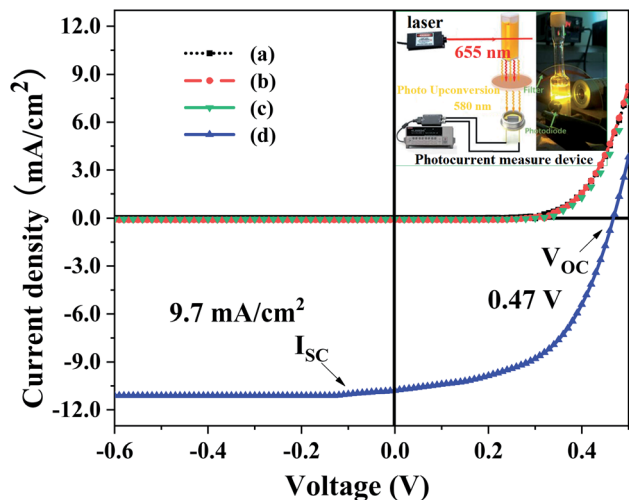


Fig. 7 Under excitation of 655 nm ($\sim 1.5 \text{ W cm}^{-2}$), I - V curve of TTA-UC powered Si-photodiode (a) dark current curve, (b) the deaerated toluene, (c) TBPCPd solution alone in deaerated toluene, (d) the TBPCPd/Rub solution in deaerated toluene). Inset: the scheme of TTA upconversion-driven Si-photodiode.

4 Conclusions

In summary, we synthesized two soluble palladium phthalocyanine complexes (TBPCPd and POPCPd) acting as the triplet sensitizers, doped with different annihilator (Rub and BPEA), respectively. Under the excitation of 655 nm diode laser ($\sim 1.5 \text{ W cm}^{-2}$), the UC efficiencies of TBPCPd/Rub (red-to-yellow), TBPCPd/BPEA (red-to-yellow) and POPCPd/BPEA (red-to-green) are at 8.03%, 1.84% and 0.07%, respectively. The TBPCPd/Rub upconversion-powered solar-cell can produce the current density of short circuit (J_{SC}) and voltage of open circuit (V_{OC}) at 9.7 mA cm^{-2} and 0.47 V, respectively, indicating that TTA red-to-yellow upconversion and solar-cell integration have potential applications.

Meanwhile, it was found that although large triplet energy-level difference ($\Delta E = {}^3E_{\text{sen.}} - {}^3E_{\text{anni.}}$) of sensitizer (${}^3E_{\text{sen.}}$)/annihilator (${}^3E_{\text{anni.}}$) pair helps to improve the upconversion, the sensitizer/annihilator pair still works when the ΔE value is less than zero and the bicomponent pair doesn't work anymore when the $\Delta E \leq -0.05 \text{ eV}$. To our best knowledge, the current study is firstly presented quantitative criteria, which can provide a simple evaluated approach for exploring the new sensitizer/annihilator pairs.

Conflicts of interest

There are no conflicts to declare.

Acknowledgements

The authors are grateful to National Natural Science Foundation of China (51873145, 51803147, 51673143), Natural Science Foundation of Jiangsu Province-Excellent Youth Foundation (No. BK20170065), Qing Lan Project of Jiangsu Province of China, 333 High-level Talents Training Project of Jiangsu Province (No. BRA2018340) and Six Talent Summits Project of Jiangsu Province (No. XCL-79) for the financial supports.

Notes and references

- 1 A. Nattestad, Y. Y. Cheng, R. W. MacQueen, T. F. Schulze, F. W. Thompson, A. J. Mozer, B. Fückel, T. Khoury, M. J. Crossley, K. Lips, G. G. Wallace and T. W. Schmidt, *J. Phys. Chem. Lett.*, 2013, **4**, 2073–2078.
- 2 V. Gray, D. Dzebo, M. Abrahamsson, B. Albinsson and K. Moth-Poulsen, *Phys. Chem. Chem. Phys.*, 2014, **16**, 10345–10352.
- 3 T. F. Schulze, Y. Y. Cheng, B. Fückel, R. W. MacQueen, A. Danos, N. J. L. K. Davis, M. J. Y. Tayebjee, T. Khoury, R. G. C. R. Clady, N. J. Ekins-Daukes, M. J. Crossley, B. Stannowski, K. Lips and T. W. Schmidt, *Aust. J. Chem.*, 2012, **65**, 480–485.
- 4 T. F. Schulze, Y. Y. Cheng, T. Khoury, M. J. Crossley, B. Stannowski, K. Lips and T. W. Schmidt, *J. Photonics Energy*, 2013, **3**, 034598.
- 5 T. F. Schulze, J. Czolk, Y.-Y. Cheng, B. Fückel, R. W. MacQueen, T. Khoury, M. J. Crossley, B. Stannowski, K. Lips, U. Lemmer, A. Colsmann and T. W. Schmidt, *J. Phys. Chem. C*, 2012, **116**, 22794–22801.
- 6 L. Frazer, J. K. Gallaher and T. W. Schmidt, *ACS Energy Lett.*, 2017, **2**, 1346–1354.
- 7 T. Dilbeck and K. Hanson, *J. Phys. Chem. Lett.*, 2018, **9**, 5810–5821.
- 8 R. S. Khnayzer, J. Blumhoff, J. A. Harrington, A. Haeefe, F. Deng and F. N. Castellano, *Chem. Commun.*, 2012, **48**, 209–211.
- 9 B. Wang, B. Sun, X. Wang, C. Ye, P. Ding, Z. Liang, Z. Chen, X. Tao and L. Wu, *J. Phys. Chem. C*, 2014, **118**, 1417–1425.
- 10 T. N. Singh-Rachford and F. N. Castellano, *Coord. Chem. Rev.*, 2010, **254**, 2560–2573.
- 11 X.-F. Zhang and W. Guo, *J. Photochem. Photobiol., A*, 2011, **225**, 117–124.
- 12 Y. Che, W. Yang, G. Tang, F. Dumoulin, J. Zhao, L. Liu and Ü. İsci, *J. Mater. Chem. C*, 2018, **6**, 5785–5793.
- 13 A. Ogunsipe, J.-Y. Chen and T. Nyokong, *New J. Chem.*, 2004, **28**, 822–827.
- 14 T. N. Singh-Rachford and F. N. Castellano, *J. Phys. Chem. A*, 2008, **112**, 3550–3556.
- 15 F. Zhong and J. Zhao, *Dyes Pigm.*, 2017, **136**, 909–918.
- 16 C. Ye, B. Wang, R. Hao, X. Wang, P. Ding, X. Tao, Z. Chen, Z. Liang and Y. Zhou, *J. Mater. Chem. C*, 2014, **2**, 8507–8514.
- 17 C. Ye, B. Sun, X. Wang, J. Yang, P. Ding, S. Zhu, Q. He, Z. Liang and X. Tao, *Dyes Pigm.*, 2014, **102**, 133–141.
- 18 Y. Y. Cheng, T. Khoury, R. G. Clady, M. J. Tayebjee, N. J. Ekins-Daukes, M. J. Crossley and T. W. Schmidt, *Phys. Chem. Chem. Phys.*, 2010, **12**, 66–71.
- 19 A. Monguzzi, J. Mezyk, F. Scotognella, R. Tubino and F. Meinardi, *Phys. Rev. B: Condens. Matter Mater. Phys.*, 2008, **78**, 195112.
- 20 A. Haeefe, J. Blumhoff, R. S. Khnayzer and F. N. Castellano, *J. Phys. Chem. Lett.*, 2012, **3**, 299–303.
- 21 C. Ye, L. Zhou, X. Wang and Z. Liang, *Phys. Chem. Chem. Phys.*, 2016, **18**, 10818–10835.
- 22 A. Turshatov, D. Busko, Y. Avlasevich, T. Miteva, K. Landfester and S. Balushev, *ChemPhysChem*, 2012, **13**, 3112–3115.

